17-Allylamino-17-demethoxygeldanamycin enhances the lethality of deoxycholic acid in primary rodent hepatocytes and established cell lines

Clint Mitchell,[1] Margaret A. Park,[1] Guo Zhang,[1,5] Song Iy Han,[1] Hisashi Harada,[2] Richard A. Franklin,[6] Adly Yacoub,[1] Pin-Lan Li,[5] Philip B. Hylemon,[4] Steven Grant,[1,2] and Paul Dent[1,3]

Departments of [1]Biochemistry, [2]Medicine, [3]Radiation Oncology, [4]Microbiology and Immunology, and [5]Pharmacology and Toxicology, Virginia Commonwealth University, Richmond, Virginia and [6]Department of Microbiology and Immunology, Brody School of Medicine, East Carolina University, Greenville, North Carolina

Abstract

Ansamycin antibiotics that target heat shock protein 90 function are being developed as anticancer agents but are also known to be dose limiting in patients due to hepatotoxicity. Herein, to better understand how the normal tissue toxicity of geldanamycins could be ameliorated to improve the therapeutic index of these agents, we examined the interactions of 17-allylamino-17-demethoxygeldanamycin (17AAG) and the secondary bile acid deoxycholic acid (DCA) in hepatocytes and fibroblasts. DCA and 17AAG interacted in a greater than additive fashion to cause hepatocyte cell death within 2 to 6 h of coadministration. As single agents DCA, but not 17AAG, enhanced the activity of extracellular signal-regulated kinase 1/2, AKT, c-Jun NH_2-terminal kinase 1/2 (JNK1/2), and p38 mitogen-activated protein kinase (MAPK). Combined exposure of cells to DCA and 17AAG further enhanced JNK1/2 and p38 MAPK activity. Inhibition of JNK1/2 or p38 MAPK, but not activator protein-1, suppressed the lethality of 17AAG and of 17AAG and DCA. Constitutive activation of AKT, but not MAPK/extracellular signal-regulated kinase kinase 1/2, suppressed 17AAG- and DCA-induced cell killing and reduced activation of JNK1/2. DCA and 17AAG exposure promoted association of BAX with mitochondria, and functional inhibition of BAX or caspase-9, but not of BID and caspase-8, suppressed 17AAG and DCA lethality. DCA and 17AAG interacted in a greater than additive fashion to promote and prolong the generation of reactive oxygen species (ROS). ROS-quenching agents, inhibition of mitochondrial function, expression of dominant-negative thioredoxin reductase, or expression of dominant-negative apoptosis signaling kinase 1 suppressed JNK1/2 and p38 MAPK activation and reduced cell killing after 17AAG and DCA exposure. The potentiation of DCA-induced ROS production by 17AAG was abolished by Ca^{2+} chelation and ROS generation, and cell killing following 17AAG and DCA treatment was abolished in cells lacking expression of PKR-like endoplasmic reticulum kinase. Thus, DCA and 17AAG interact to stimulate Ca^{2+}-dependent and PKR-like endoplasmic reticulum kinase–dependent ROS production; high levels of ROS promote intense activation of the p38 MAPK and JNK1/2 pathways that signal to activate the intrinsic apoptosis pathway. [Mol Cancer Ther 2007;6(2):618–32]

Introduction

Heat shock protein 90 (HSP90) is a member of a class of proteins referred to as molecular chaperones. HSP90 controls the folding of proteins, particularly those involved in signal transduction and cell survival (1). When HSP90 function is inhibited, many proteins become improperly folded and are then targeted for degradation, including ERBB1, ERBB2, Raf-1, activated B-Raf, AKT, and steroid receptors (e.g., refs. 2, 3). All of these proteins play key roles in growth and cell survival in tumor cells, arguing that loss of HSP90 function could have pleiotropic effects on cell biology. Several HSP90 inhibitors have been developed as chemotherapeutic agents, such as the ansamycin antibiotics, including geldanamycin and its analogues [e.g., 17-allylamino-17-demethoxygeldanamycin (17AAG); NSC 330507; refs. 4–10].

Geldanamycin was originally described 30 years ago as an antibiotic of the benzoquinoid ansamycin group (11). Interactions between this family of drugs and the NH_2 terminus of HSP90 interfere with the functional binding of HSP90 to other proteins, thereby both inhibiting the function of protective kinase activities (e.g., Raf-1 and AKT) as well as causing an unfolded protein response due to protein denaturation and ubiquination (12, 13). One potential additional HSP90-independent effect of geldanamycins has been argued to be the generation of reactive oxygen species (ROS) in cells (4, 5, 14). HSP90 antagonists,

Received 8/28/06; revised 11/30/06; accepted 12/6/06.

Grant support: Public Health Service grants R01-CA88906, R01-DK52825, and P01-CA104177 (P. Dent) and P01-CA72955, R01-CA63753, and R01-CA77141 (S. Grant); Department of Defense Awards BC020338 and DAMD17-03-1-0262 (P. Dent); Leukemia Society of America grant 6405-97 (S. Grant); and The Jim Valvano ''V'' Foundation. P. Dent is the holder of the Universal, Inc. Professorship in Signal Transduction Research.

The costs of publication of this article were defrayed in part by the payment of page charges. This article must therefore be hereby marked *advertisement* in accordance with 18 U.S.C. Section 1734 solely to indicate this fact.

Requests for reprints: Paul Dent, Department of Biochemistry, Massey Cancer Center, Box 980035, Virginia Commonwealth University, Richmond, VA 23298-0035. Phone: 804-628-0861; Fax: 804-827-1309. E-mail: pdent@vcu.edu

doi:10.1158/1535-7163.MCT-06-0532

such as 17AAG, have also been shown to enhance the lethal effects of cytotoxic drugs, such as paclitaxel, which may be in part due to reduced function of cytoprotective signaling pathway functions (15, 16). *In vivo*, geldanamycin was found to have dose-limiting toxicity due to liver damage; newer more soluble derivatives of geldanamycin that also have lower HSP90 inhibitory effects (e.g., 17AAG and 17-dimethylaminoethylamino-17-demethoxygeldanamycin) are under phase II trial in the clinic, although these agents also have been noted to have hepatotoxicity (17–19). Free plasma concentrations of 17AAG in patients have been noted to be in the low 1 to 5 μmol/L range for up to 12 h after drug infusion, which is significantly higher than the required concentration of drug to inhibit HSP90 function (19). Many established therapeutic agents have also been shown to have varying toxicities in the liver, both killing hepatocytes and causing cholestasis, including 1-β-D-arabinofuranosylcytosine (20), arsenic trioxide (21), and platinum drugs (22).

Bile acids are detergent molecules, synthesized from cholesterol in the liver, which are released into the gut on feeding and are essential for digestion. Bile acids, after feeding, reenter the liver via the portal vein together with digested nutrients and are recirculated back into the gall bladder for use during the next feeding cycle (23). Individually, when retained within the liver because of impaired secretion into the bile canaliculi, bile acids also have hepatocellular toxicity both *in vivo* and *in vitro*, effects that have been linked to prolonged elevation of ROS and ceramide levels (24–27). We have reported that treatment of primary hepatocytes with the secondary bile acid generated by bacteria in the colon, deoxycholic acid (DCA), a putative tumor promoter, caused activation of ERBB1, which was responsible for activation of the extracellular signal-regulated kinase (ERK) 1/2 and, to a lesser extent, AKT pathways (25–27). In addition to ERBB1, bile acids induce activation of the insulin receptor in primary rodent hepatocytes (28). Activation of the phosphatidylinositol 3-kinase (PI3K)/AKT pathway by DCA was more strongly linked to activation of the insulin receptor than to activation of ERBB1. DCA-induced generation of ROS in hepatocytes was responsible for inhibition of protein tyrosine phosphatase function and activation of receptor tyrosine kinases. ROS scavengers blocked the suppression of protein tyrosine phosphatase activity as well as activation of receptor tyrosine kinases; several studies by other laboratories have argued that protein tyrosine phosphatase activity is sensitive to cellular redox status (29). Blockade of DCA-induced ERK1/2 or PI3K activation increased hepatocyte apoptosis (25–27). In these studies, apoptosis was dependent on bile acid– and ceramide-induced, ROS- and ligand-independent activation of the FAS receptor (CD95). Bile acids activate the FAS receptor/c-Jun NH_2-terminal kinase (JNK) 1/2 pathway via acidic sphingomyelinase/ceramide generation (30). Other groups have also noted that bile acids can activate ERBB1 and the FAS receptor (e.g., refs. 31, 32).

As both bile acids and 17AAG can generate ROS, the present studies were done to examine the mechanism(s), specifically prolonged high levels of ROS generation, by which bile acids and geldanamycins combined interact to alter hepatocyte viability and, if so, whether we could propose a rational basis for ameliorating the hepatotoxicity of geldanamycins and improving the therapeutic index for this class of agents.

Materials and Methods

Materials

All bile acids and CHAPS were obtained from Sigma Chemical Co. (St. Louis, MO). Phosphorylated/total ERK1/2, phosphorylated/total JNK1/2, phosphorylated/total p38 mitogen-activated protein kinase (MAPK), anti-S473 AKT, and total AKT antibodies were purchased from Cell Signaling Technology (Worcester, MA). All the secondary antibodies [anti-rabbit horseradish peroxidase, anti-mouse horseradish peroxidase, and anti-goat horseradish peroxidase] were purchased from Santa Cruz Biotechnology (Santa Cruz, CA). Src family kinase inhibitor (PP2), JNK inhibitor peptide, and ERBB1 inhibitor (AG1478) were supplied by Calbiochem (San Diego, CA) as powder, dissolved in sterile DMSO, and stored frozen under light-protected conditions at −80°C. Enhanced chemiluminescence kits were purchased from Amersham (Bucks, United Kingdom) and NEN Life Science Products (Boston, MA). Trypsin-EDTA, Williams' medium E, and penicillin-streptomycin were purchased from Life Technologies (Grand Island, NY). The geldanamycin 17AAG was purchased from Calbiochem. Fluo-3 was purchased from Molecular Probes (Eugene, OR) and dissolved in DMSO. BAX/BAK$^{-/-}$ and BID$^{-/-}$ fibroblasts were kindly provided by Dr. S. Korsmeyer (Harvard University, Boston, MA). Transformed PKR-like endoplasmic reticulum (ER) kinase (PERK$^{-/-}$) cells were a kind gift from the Ron Laboratory, Skirball Institute, New York University School of Medicine (New York, NY). The dominant-negative p38 MAPK and activated MAPK/ERK kinase 1 EE adenoviruses were kindly provided by Dr. K. Valerie (Virginia Commonwealth University, Richmond, VA) and Dr. J. Moltken (University of Cincinnati, Cincinnati, OH), respectively. HeLa cells expressing thioredoxin reductase expression plasmids were kindly provided by Dr. David Gius (Radiobiology Branch, National Cancer Institute, Bethesda, MD). Other reagents were of the highest quality commercially available (25–28).

Methods

Primary Culture of Rodent Hepatocytes

Hepatocytes were isolated from adult male Sprague-Dawley rats or C57/BL6 mice by the two-step collagenase perfusion technique. Acidic sphingomyelinase–null mice were kindly supplied by Dr. R. Kolesnik (Memorial Sloan-Kettering Cancer Center, New York, NY). FAS receptor–null mice were purchased from The Jackson Laboratory (Bar Harbor, ME). The isolated hepatocytes were plated on rat-tail collagen (Vitrogen)-coated plate at a density of 2×10^5 cells per well and cultured in serum-free DMEM supplemented with 0.1 μmol/L dexamethasone, 1 μmol/L thyroxine, and 100 μg/mL of penicillin/streptomycin at 37°C in a humidified atmosphere containing 5% CO_2. A

medium change was done 3 h after plating. Unless otherwise indicated, cells were treated with 50 μmol/L of DCA or 17AAG ~24 h after isolation.

Cell Treatments, SDS-PAGE, and Western Blot Analysis

Cells were treated with either 17AAG (0.1–3.0 μmol/L) or 17-dimethylaminoethylamino-17-demethoxygeldanamycin (0.1–3.0 μmol/L) 5 min before bile acid addition. Unless otherwise stated in the figure legend, cells were treated with 17AAG (1 μmol/L), which is well within the clinical range for this drug within 6 h of infusion (3–10 μmol/L; refs. 9, 10). Cells were then exposed to DCA (50 μmol/L). DCA (50 μmol/L) was chosen for the majority of these studies as it is within the reference range of bile acid levels in the liver as well as to observe large statistically significant alterations in hepatocyte biological behavior. For SDS-PAGE and immunoblotting, hepatocytes were lysed in a nondenaturing lysis buffer and prepared for immunoprecipitation as described in refs. 25–27 or in whole-cell lysis buffer [0.5 mol/L Tris-HCl (pH 6.8), 2% SDS, 10% glycerol, 1% β-mercaptoethanol, 0.02% bromphenol blue], and the samples were boiled for 30 min. After immunoprecipitation, samples were boiled in whole-cell lysis buffer. The boiled samples were loaded onto 10% to 14% SDS-PAGE, and electrophoresis was run overnight. Proteins were electrophoretically transferred onto 0.22-μm nitrocellulose and immunoblotted with various primary antibodies against different proteins. All immunoblots were visualized by enhanced chemiluminescence. For presentation, immunoblots were digitally scanned at 600 dpi using Adobe PhotoShop 7.0 and their color was removed and figures were generated in Microsoft PowerPoint. Densitometric analysis for enhanced chemiluminescence immunoblots was done using a Fluorochem 8800 Image System and the respective software (Alpha Innotech Corp., San Leandro, CA), and band densities were normalized to that of a total protein loading control.

Poly-L-Lysine Adenoviral Vectors and Recombinant Adenoviral Vectors: Generation and Infection **In vitro**

Two adenoviral technologies were used. Replication-defective adenovirus is conjugated to poly-L-lysine and cDNA plasmid constructs to express a dominant-negative caspase-8 and dominant-negative FAS-associated death domain proteins as described in refs. 25–28. Second, we generated and purchased previously noted recombinant adenoviruses to express constitutively activated and dominant-negative AKT and MEK1 proteins, dominant-negative ERBB1 (COOH-terminal 533-amino acid deletion; CD533), dominant-negative caspase-9, dominant c-Jun (TAM67), and BCL-$_{XL}$ (Vector Biolabs, Philadelphia, PA). Hepatocytes were transfected/infected with these adenoviruses at approximate multiplicities of infection (MOI) of 250 and 30, respectively. Cells were further incubated for 24 h to ensure adequate expression of transduced gene products before drug exposures.

Morphologic Detection of Apoptosis by Wright-Giemsa Assays

Morphologic assessment of apoptosis was done as follows (25–28). Hepatocytes were harvested by trypsinization with trypsin-EDTA for ~10 min at 37°C. As some apoptotic cells detached from the culture substratum into the medium, these cells were also collected by centrifugation of the medium at 1,500 rpm for 5 min. The pooled cell pellets were resuspended, and a fraction of the suspension was centrifuged in a cytospinner (Cytospin 3, Shandon, Inc., Pittsburgh, PA). For Wright-Giemsa staining, the slides were fixed and stained in Diff-Quik Stain Set (Dade Diagnostics of P.P., Inc., Aguada, Puerto Rico) according to the manufacturer's instruction and viewed under a light microscope. Nuclear and total cellular morphology was evaluated. Giemsa staining was used to identify total cell numbers and total numbers of apoptotic and nonapoptotic manifestations of cell killing. Five hundred cells from several randomly chosen fields were counted, and the number of apoptotic cells was counted and expressed as a percentage of the total number of cells counted.

Generation of Rho 0 HuH7 Cells

HuH7.Ntcp human hepatoma cells (kindly provided by Dr. G. Gores, Mayo Clinic, Rochester, MN) were cultured in DMEM containing 10% (v/v) FCS (27). To generate HuH7.Ntcp Rho 0 cells, HuH7.Ntcp cells were cultured in DMEM containing 10% (v/v) FCS, 50 μg/mL uridine, 1 mmol/L sodium pyruvate, and the growth medium supplemented (for Rho 0 cell generation) with 10 μg/mL ethidium bromide. Cells were cultured in this medium or in parallel in growth medium without ethidium bromide for 8 weeks before any further experimentation. Removal of uridine and pyruvate from the growth medium of established HuH7 Rho 0 cells resulted in rapid (~24–48 h) growth arrest and cell death (data not shown; ref. 26).

Assessment of ROS/Reactive Nitrogen Species Generation

Hepatocytes were plated in 96-well plates. Dihydro-DCF is sensitive to oxidation by hydroxyl radicals and peroxynitrite directly and hydrogen peroxide in the presence of a peroxidase. Fluorescence measurements were obtained 0 to 60 min after DCA and 17AAG addition, at the indicated concentrations, with a Packard FluoroCount plate reader. Ten minutes before the measurement of ROS in the plate reader, cells were incubated with dihydro-DCF (5 μmol/L) or DMSO vehicle, which is nonfluorescent in its dihydro form but, on reaction with ROS/reactive nitrogen species, becomes highly fluorescent (26). Medium was then rapidly changed to medium lacking dye (in the dark), and the plate was placed into the plate reader. Data at each time point are presented corrected for basal fluorescence of vehicle-treated cells at the same time point. Each time point represents the mean of eight data points per experiment and of a total of three independent experiments.

Assessment of Ceramide Generation

Lipids were extracted, and mass amounts of ceramide in cellular extracts were measured by the diacylglycerol kinase enzymatic method (33). Briefly, hepatocytes were washed with PBS and scraped into 1 mL of cold methanol containing 2.5 μL of concentrated HCl. Lipids were extracted by adding 2 mL chloroform and 1 mol/L NaCl (1:1, v/v), and phases were separated. An aliquot (100 μL)

of the chloroform phase was dried under nitrogen gas. Bovine brain type III ceramide was used as a standard. The enzymatic reaction was started by the addition of 100 μL of 50 mmol/L imidazole, 1 mmol/L diethylenetriaminepenta acetic acid, 12.5 mmol/L $MgCl_2$, 50 mmol/L NaCl, 1 mmol/L EGTA, 10 mmol/L DTT, 1 mmol/L ATP, 1.5% *N*-octyl-D-glucopyranoside, 1 mmol/L cardiolipin, 0.01 unit of diacylglycerol kinase, and 1 μCi [γ-^{32}P]ATP. After incubation at 37°C for 35 min, with 15 min of sonication at room temperature in between, lipids were extracted by the addition of 500 μL of chloroform/methanol/HCl (100:100:1) and 100 μL of 1 mol/L NaCl. Labeled ceramide 1-phosphate and phosphatidic acid (50 μL organic layer) were resolved by TLC with chloroform/acetone/methanol/acetic acid/water (10:4:3:2:1). Bands corresponding to ceramide were quantified with a Bio-Rad (Hercules, CA) phosphorimager.

Assessment of Cytosolic Ca^{2+} Levels

Method 1. Cells (100 μL, 2.5 × 10^5/mL) in DMEM containing 10% FCS, 2 mmol/L glutamine, 100 units/mL penicillin, and 100 μg/mL streptomycin were placed in a 96-well microtiter plates and allowed to adhere overnight. The next morning, the medium was removed by inverting the plate on paper towels, and 100 μL HBSS containing 1.5 μmol/L Fluo-3, 0.02% (v/v) F-127 (Molecular Probes), 1% (v/v) FCS, and 2 mmol/L probenecid (Sigma Chemical) was added to the wells. The Fluo-3 was reconstituted as follows: a 50 μg vial of Fluo-3 was reconstituted in 25 μL DMSO containing 20% (v/v) F-127 and vortexed. To this, 113 μL of fetal bovine serum were added to this mix and the vial was vortexed again. Then, 5 μL of the reconstituted Fluo-3 were added per mL of HBSS containing 1% FCS and 2 mmol/L probenecid and used to label the cells. Cells were incubated for 30 min with the dye and washed once (by inversion on a paper towel) and resuspended in HBSS containing 1% (v/v) FCS and 2 mmol/L probenecid. The microplates were then allowed to incubate for 15 min to insure the hydrolysis of the dye ester. Following this incubation, cells were washed again and resuspended in HBSS containing 1% (v/v) FCS and 2 mmol/L probenecid and used for calcium measurements. Cells were stimulated as indicated in the figures, and the fluorescence was monitored over time on a Bio-Tek FL600 fluorescence/absorbance spectophotometer (Bio-Tek, Winooski, VT). The wavelength for excitation was 485 nm and emission was measured at 530 nm. The HBSS contained Mg^{2+} and Ca^{2+} but did not contain phenol red.

Method 2. A high-speed wavelength switching fluorescence image analysis system (MetaFluor) was used to determine $[Ca^{2+}]_i$ in the mouse embryonic fibroblasts (MEF), seeded on the four-well chamber with a transparent bottom (Lab-Tek), with fura-2 acetoxymethyl ester (fura-2) as an indicator. After loading with 10 μmol/L fura-2 at room temperature for 50 min, the cells were washed thrice with Hanks' buffer containing 137 mmol/L NaCl, 5.4 mmol/L KCl, 4.2 mmol/L $NaHCO_3$, 3 mmol/L Na_2HPO_4, 0.4 mmol/L KH_2PO_4, 1.5 mmol/L $CaCl_2$, 0.5 mmol/L $MgCl_2$, 0.8 mmol/L $MgSO_4$, 10 mmol/L glucose, and 10 mmol/L HEPES (pH 7.4). Then, 17AAG (3 μmol/L), DCA (50 μmol/L), or combination of 17AAG (3 μmol/L) and DCA (50 μmol/L) was added into the bath solution to stimulate the MEFs, respectively. A fluorescence ratio of excitation at 340 nm to that at 380 nm (F340/F380) was determined after background subtraction. The ratio of fura-2 emissions, when excited at the wavelengths of 340 and 380 nm, was recorded with a digital camera (Nikon Diaphoto TMD Inverted Microscope, Melville, NY). MetaFluor imaging and analysis software were used to acquire, digitize, and store the images for off-line processing and statistical analysis (Universal Imaging, Sunnyvale, CA).

Data Analysis

Comparison of the effects of various treatments, including Western blot analysis and cell death determinations, was done using one-way ANOVA and a two-tailed Student's *t* test. Differences with a *P* value of <0.05 were considered statistically significant. Experiments shown are the means of multiple individual points (±SE).

Results

Initial studies examined the killing of primary rat hepatocytes exposed for 4 h to DCA (50 μmol/L) and 17AAG (0.03–3.0 μmol/L) as single agents and in combination. Treatment of hepatocytes with 50 μmol/L DCA very weakly promoted cell killing, whereas treatment with 17AAG at all concentrations promoted a modest to strong induction of cell death (Fig. 1). The earliest manifestation of enhanced cell killing was noted ~2 h after exposure (data not shown). Combined exposure of hepatocytes to 17AAG

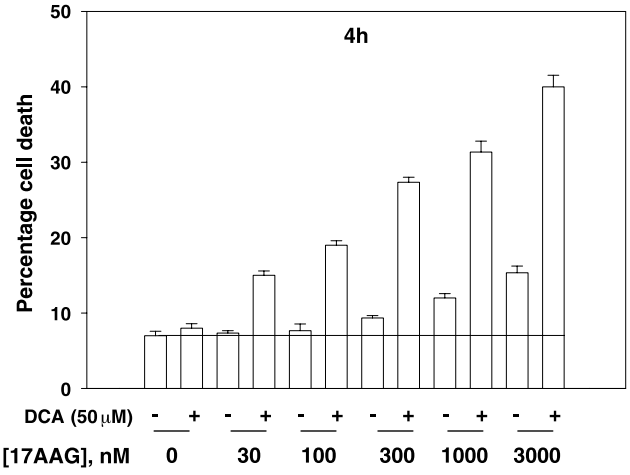

Figure 1. DCA enhances the lethality of 17AAG in primary rat hepatocytes in a dose-dependent manner. Primary rat hepatocytes were cultured as in Materials and Methods in 12-well plates and, 24 h after plating, treated where appropriate with vehicle (DCA, PBS; 17AAG, DMSO), 17AAG (0–3 μmol/L), DCA (50 μmol/L), or the combination of the agents. Cells were isolated by trypsinization 4 h after DCA/17AAG exposure and spun onto glass slides. Cells were Wright-Giemsa stained, and the total number of dead (apoptotic and necrotic) cells was determined as a percentage of all cells counted. *Columns,* each assay was done in triplicate and the data are from a representative study from a series done by two different individuals ($n = 3$); *bars,* SE.

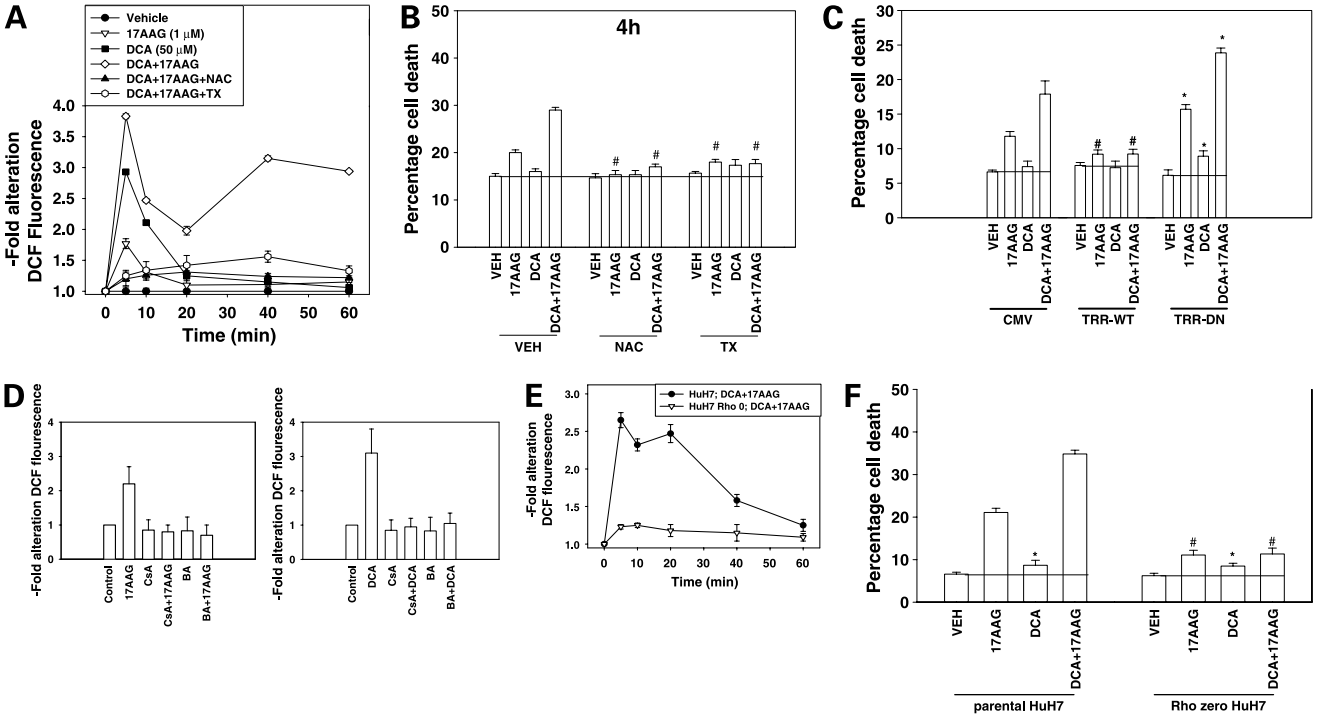

Figure 2. DCA and 17AAG interact to cause enhanced and prolonged generation of ROS that is causal in the synergistic cell killing effect. **A,** primary rat hepatocytes were cultured as in Materials and Methods in 96-well plates and, 24 h after plating, simultaneously treated where appropriate with vehicle (DCA, PBS; 17AAG, DMSO), 17AAG (1 μmol/L), DCA (50 μmol/L), or the combination of the agents. In parallel studies, cells were pretreated where indicated with either NAC (20 mmol/L) or Trolox (*TX*; 10 μmol/L). Fifteen minutes before each indicated time point, DCFH was added to the culture medium as described in Materials and Methods. Medium containing the dye was removed after 15 min, and fresh medium that did not contain any agent was added. Plates were immediately placed into an appropriate plate reader to determine DCFH fluorescence. *Points,* mean of eight separate determinations from one representative experiment ($n = 3$); *bars,* SE. **B,** primary rat hepatocytes were cultured as in Materials and Methods in 12-well plates and, 24 h after plating, treated with vehicle (*VEH*; DMSO), NAC (20 mmol/L), or Trolox (10 μmol/L). Thirty minutes after NAC/Trolox treatment, hepatocytes were treated with vehicle (DCA, PBS; 17AAG, DMSO), 17AAG (1 μmol/L), DCA (50 μmol/L), or the combination of the agents. Cells were isolated by trypsinization 4 h after DCA exposure and spun onto glass slides. Cells were stained with Wright-Giemsa, and the total number of dead (apoptotic and necrotic) cells was determined as a percentage of all cells counted. *Columns,* each assay was done in triplicate and the data are from a representative study done by two different individuals ($n = 3$); *bars,* SE. #, $P < 0.05$, less than corresponding treatment value in vector-transfected cells. **C,** HeLa cells were cultured as described in Materials and Methods and, 24 h after plating, simultaneously treated where appropriate with vehicle (DCA, PBS; 17AAG, DMSO), 17AAG (1 μmol/L), DCA (50 μmol/L), or the combination of the agents. Cells were isolated 12 h after drug exposure and spun onto glass slides. Cells were stained with Wright-Giemsa, and the total number of dead (apoptotic and necrotic) cells was determined as a percentage of all cells counted. Each assay was done in triplicate. *Columns,* mean of four separate experiments; *bars,* SE. *, $P < 0.05$, greater than corresponding treatment value in vector-transfected cells; #, $P < 0.05$, less than corresponding treatment value in vector-transfected cells. **D** and **E,** primary hepatocytes (**D**) or HuH7 cells (**E**) were cultured as in Materials and Methods in 96-well plates and, 24 h after plating, simultaneously treated where appropriate with vehicle (DCA, PBS; 17AAG, DMSO), 17AAG (1 μmol/L), DCA (50 μmol/L), or the combination of the agents. For studies using cyclosporin A (*CsA*; 1 μmol/L) or bongkrekic acid (*BA*; 50 μmol/L), cells were pretreated before 17AAG/DCA exposure for 15 min. Fifteen minutes before each indicated time point, DCFH was added to the culture medium as described in Materials and Methods. Medium containing the dye was removed, and fresh medium that did not contain any agent was added. Plates were immediately placed into an appropriate plate reader to determine DCFH fluorescence. *Points,* mean of eight separate determinations from one representative experiment ($n = 3$); *bars,* SE. **F,** HuH7 cells and HuH7 Rho 0 cells were cultured as in Materials and Methods in 12-well plates and, 24 h after plating, treated with vehicle (DCA, PBS; 17AAG, DMSO), 17AAG (1 μmol/L), DCA (50 μmol/L), or the combination of the agents. Cells were isolated by trypsinization 12 h after DCA/17AAG exposure and spun onto glass slides. Cells were stained with Wright-Giemsa, and the total number of dead (apoptotic and necrotic) cells was determined as a percentage of all cells counted. *Columns,* each assay was done in triplicate and the data are the mean of five separate studies; *bars,* SE. #, $P < 0.05$, less than corresponding treatment value in parental cells; *, $P < 0.05$, greater than vehicle control – treated cells.

and DCA resulted in a significantly greater than additive induction of cell killing above that induced by either agent alone. Similar data with DCA and 17AAG were obtained in primary human hepatocytes (data not shown).

Both DCA and geldanamycins have been shown to induce production of ROS in primary hepatocytes and in other established cell types, respectively, and we next examined whether DCA and 17AAG interacted to modulate ROS levels in hepatocytes. As individual agents, both DCA and 17AAG enhanced ROS levels in primary rat hepatocytes (Fig. 2A). Combined exposure of hepatocytes to DCA and 17AAG enhanced ROS production above that generated by each agent individually, and in addition, combined treatment with both agents prolonged the duration of ROS production. The production of ROS was suppressed by inclusion of the quenching agents *N*-acetyl cysteine (NAC) and Trolox. Based on these observations, we then determined whether the elevated

levels of ROS production were responsible for the enhanced levels of cell killing. Incubation of hepatocytes with either NAC or Trolox reduced 17AAG lethality and also abolished the greater than additive induction of cell killing caused by combined DCA and 17AAG treatment (Fig. 2B).

Based on the findings in Fig. 2A and B, we then used molecular tools to confirm our data using small-molecule ROS-quenching agents. When active and mutated inactive forms of thioredoxin reductase were stably overexpressed in cervical carcinoma (HeLa) cells treated with DCA and 17AAG, tumor cell survival was enhanced by expression of wild-type thioredoxin reductase and decreased by expression of mutated thioredoxin reductase, which is in general agreement with our primary hepatocyte data using NAC (Fig. 2C). Previous analyses from our group have shown that DCA promotes ROS generation in hepatocytes and hepatoma cells, which is dependent in part on the presence of functional mitochondria. ROS generation induced by DCA and 17AAG was suppressed in primary rat hepatocytes incubated with inhibitors of mitochondrial respiration and was reduced in human HuH7 hepatoma cells lacking functional mitochondria (Rho 0 cells; Fig. 2D and E). Loss of mitochondrial ROS production suppressed the lethality of DCA and 17AAG in Rho 0 HuH7 cells lacking functional mitochondria (Fig. 2F). The reduced lethality observed after drug exposure in Rho 0 cells may also be due, in a general mechanistic sense, to reduced expression of mitochondrial proapoptotic effectors (e.g., cytochrome *c*). Collectively, these findings argue that ROS generation plays an important role in 17AAG lethality in both primary hepatocytes and transformed cells, including hepatoma cells.

Prolonged exposure of tumor cell lines to 17AAG (12–24 h) has been shown to inhibit HSP90 function, leading to reduced expression of prosurvival HSP90 client signal transduction proteins, such as ERBB1, ERBB2, AKT, Raf-1, and B-Raf. Several of these prosurvival signaling proteins in primary hepatocytes are activated by DCA, including ERBB1, ERBB2, Raf-1, and AKT, and inhibition of these kinases had previously been shown by ourselves and others to promote bile acid toxicity (25–27). As such, we determined whether ERK1/2 and AKT, as well as the stress-activated MAPK pathways JNK1/2 and p38 MAPK, were activated following DCA and 17AAG exposure. Treatment of primary rat hepatocytes with DCA activated MEK1/2, ERK1/2, AKT, JNK1/2, and, to a lesser extent, p38 MAPK (Fig. 3A–C). Treatment of rat hepatocytes with 17AAG as a single agent did not significantly alter the phosphorylation of these kinase proteins in primary rat hepatocytes within the 6-h time frame of our study. To our surprise, short-term exposure of hepatocytes to DCA and 17AAG promoted a more prolonged intense activation of JNK1/2 and p38 MAPK (2 h after exposure, to a lesser extent at the 4- and 6-h time points) and also of ERK1/2 and AKT (2 h after exposure) without altering activation status of ERK1/2 or AKT 4 or 6 h after treatment. In rat hepatocytes, DCA-induced activation of ERK1/2 remained elevated for up to 6 h, whereas the activation of AKT had dissipated 4 to 6 h after exposure.

To further illustrate our above immunoblotting data, 2 h after exposure, DCA activated JNK1/2 2.7 $\pm$ 0.5–fold above basal levels, whereas 17AAG did not alter JNK1/2 activity. Combined exposure to DCA and 17AAG activated JNK1/2 6.2 $\pm$ 0.8–fold above basal levels; this represents a 3.1-fold increase in DCA-stimulated JNK1/2 activity caused by 17AAG coexposure ($n = 3$; $P < 0.05$ greater activation for the combined exposure than the fold activation induced by either agent alone). With respect to p38 MAPK activation, 2 h after exposure, DCA activated p38 MAPK 1.9 $\pm$ 0.4–fold above basal levels, whereas 17AAG did not significantly activate p38 MAPK. Combined exposure to DCA and 17AAG activated p38 MAPK 3.5 $\pm$ 0.4–fold above basal levels; this represents a 2.8-fold increase in DCA-stimulated p38 MAPK activity caused by 17AAG coexposure ($n = 3$; $P < 0.05$ greater activation for the combined exposure than the fold activation induced by either agent alone). Collectively, these findings show that 17AAG and DCA interact to rapidly promote JNK1/2 and p38 MAPK activation above that induced by DCA as a single agent.

Prolonged intense activation of the JNK1/2 and p38 MAPK pathways in many cell types has been linked to the promotion of cell death. In hepatocytes, we and others have shown that JNK1, but not JNK2, is linked to death signaling by bile acids and other ROS-generating agents (e.g., refs. 26, 27). Expression of dominant-negative p38α MAPK or expression of dominant-negative JNK1 suppressed the induction of cell death by 17AAG and by combined DCA and 17AAG exposure (Fig. 3D). In contrast to expression of dominant-negative JNK1, expression of dominant-negative c-Jun (TAM67) enhanced DCA lethality but had a no significant effect on the amount of cell killing observed in cells exposed to DCA and 17AAG (Fig. 3E). This suggests that the JNK1/2 pathway, but not c-Jun/activator protein-1 signaling, is involved in promoting DCA and 17AAG lethality.

In general agreement with the fact that AKT activity dissipated more rapidly than that of ERK1/2 after 17AAG and DCA treatment, expression of constitutively active AKT modestly enhanced cell survival following drug exposure, which correlated with suppression of the overall levels of JNK1/2 activation but not those of p38α MAPK (Fig. 3F). In general agreement with the fact that AKT activity dissipated more rapidly than that of ERK1/2, and that ERK1/2 activity remained elevated for up to 6 h, expression of dominant-negative MEK1 promoted 17AAG- and DCA-induced cell death, whereas expression of dominant-negative AKT did not further enhance the toxicity of 17AAG and DCA exposure (Fig. 3G). Of note, dominant-negative MEK1 enhanced the lethality of 17AAG as a single agent, although 17AAG did not appreciably activate ERK1/2, in general agreement with our findings in hepatoma and leukemia cell types using the MEK1/2

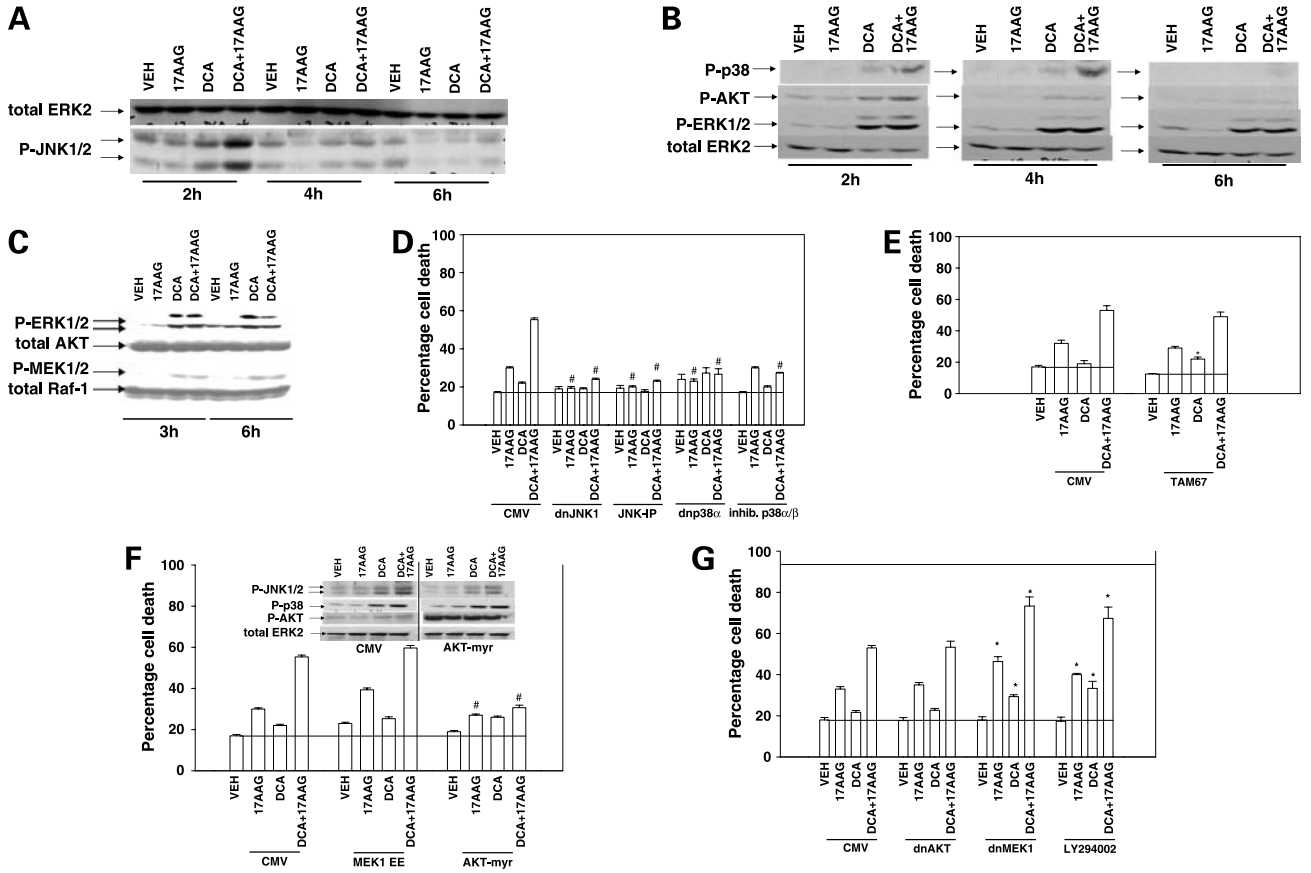

Figure 3. Exposure to DCA and 17AAG promotes greater short-term activation of JNK1/2, p38 MAPK, and ERK1/2 in primary rat hepatocytes. **A** and **B,** primary rat hepatocytes were cultured as in Materials and Methods in 12-well plates and, 24 h after plating, treated where appropriate with vehicle (DCA, PBS; 17AAG, DMSO), 17AAG (1 μmol/L), DCA (50 μmol/L), or the combination of the agents. Cells were lysed in SDS-PAGE sample buffer at the indicated times, and following SDS-PAGE and transfer to nitrocellulose, immunoblotting was done to determine the phosphorylation (activity) status of ERK1/2, AKT (S473), p38 MAPK, and JNK1/2. Data are from a series of experiments ($n = 5$). **C,** primary rat hepatocytes were cultured as in Materials and Methods in 12-well plates and, 24 h after plating, treated where appropriate with vehicle (DCA, PBS; 17AAG, DMSO), 17AAG (1 μmol/L), DCA (50 μmol/L), or the combination of the agents. Cells were lysed in SDS-PAGE sample buffer at the indicated times, and following SDS-PAGE and transfer to nitrocellulose, immunoblotting was done to determine the phosphorylation (activity) status of ERK1/2 and MEK1/2 and the expression (total protein) of Raf-1 and AKT. Data are from a series of experiments ($n = 3$). **D,** primary rat hepatocytes were cultured as in Materials and Methods in 12-well plates and, 4 h after plating, infected (50 MOI) with control [cytomegalovirus (*CMV*)] recombinant adenovirus, dominant-negative JNK1 virus (*dnJNK1*), or dominant-negative p38α MAPK virus (*dnp38α*). Twenty-four hours after infection, cells were treated with vehicle (DMSO), JNK inhibitor peptide (*JNK-IP*; 10 μmol/L), or the p38α/β MAP inhibitor SB203580 (*inhib. p38α/β*; 1 μmol/L). Thirty minutes after SB203580 treatment, cells were exposed to vehicle (DCA, PBS; 17AAG, DMSO), 17AAG (1 μmol/L), DCA (50 μmol/L), or the combination of the agents. Cells were isolated by trypsinization 4 h after DCA/17AAG exposure and spun onto glass slides. Cells were stained with Wright-Giemsa, and the total number of dead (apoptotic and necrotic) cells was determined as a percentage of all cells counted. *Columns,* assay done in triplicate ($n = 3$); *bars,* SE. #, $P < 0.05$, less than corresponding treatment value in vector-transfected cells. **E,** primary rat hepatocytes were cultured as in Materials and Methods in 12-well plates and, 4 h after plating, infected (50 MOI) with control (*CMV*) recombinant adenovirus or a virus to express dominant-negative c-Jun (*TAM67*). Twenty-four hours after infection, cells were treated with vehicle (DCA, PBS; 17AAG, DMSO), 17AAG (1 μmol/L), DCA (50 μmol/L), or the combination of the agents. Cells were isolated by trypsinization 4 h after DCA/17AAG exposure and spun onto glass slides. Cells were stained with Wright-Giemsa, and the total number of dead (apoptotic and necrotic) cells was determined as a percentage of all cells counted. *Columns,* each assay was done in triplicate and the data are from a representative study done by two different individuals ($n = 3$); *bars,* SE. *, $P < 0.05$, greater than corresponding treatment value in vector-transfected cells. **F,** primary rat hepatocytes were cultured as in Materials and Methods in 12-well plates and, 4 h after plating, infected (50 MOI) with control (*CMV*) recombinant adenovirus, active MEK1 EE virus, or an active myr-AKT virus. Twenty-four hours after infection, cells were treated with vehicle (DCA, PBS; 17AAG, DMSO), 17AAG (1 μmol/L), DCA (50 μmol/L), or the combination of the agents. Cells were isolated by trypsinization 4 h after DCA/17AAG exposure and spun onto glass slides. Cells were stained with Wright-Giemsa, and the total number of dead (apoptotic and necrotic) cells was determined as a percentage of all cells counted. *Columns,* each assay was done in triplicate and the data are from a representative study done by two different individuals ($n = 3$); *bars,* SE. #, $P < 0.05$, less than corresponding treatment value in vector-transfected cells. *Inset,* cells infected with control CMV or active myr-AKT virus were isolated 4 h after DCA and 17AAG exposure and immunoblotting was done to determine the phosphorylation status of AKT (S473), JNK1/2, and p38 MAPK. **G,** primary rat hepatocytes were cultured as in Materials and Methods in 12-well plates and, 4 h after plating, infected (50 MOI) with control (*CMV*) recombinant adenovirus, dominant-negative MEK1 (*dnMEK1*) virus, or a dominant-negative AKT (*dnAKT*) virus. Twenty-four hours after infection, cells were treated with vehicle (DCA, PBS; 17AAG, DMSO), 17AAG (1 μmol/L), DCA (50 μmol/L), or the combination of the agents. As indicated, 24 h after CMV infection, cells were treated with vehicle (DMSO) or the PI3K inhibitor LY294002 (10 μmol/L). Cells were isolated by trypsinization 4 h after DCA/17AAG exposure and spun onto glass slides. Cells were stained with Wright-Giemsa, and the total number of dead (apoptotic and necrotic) cells was determined as a percentage of all cells counted. *Columns,* each assay was done in triplicate and the data are from a representative study done by two different individuals ($n = 3$); *bars,* SE. *, $P < 0.05$, greater than corresponding treatment value in vector-transfected cells.

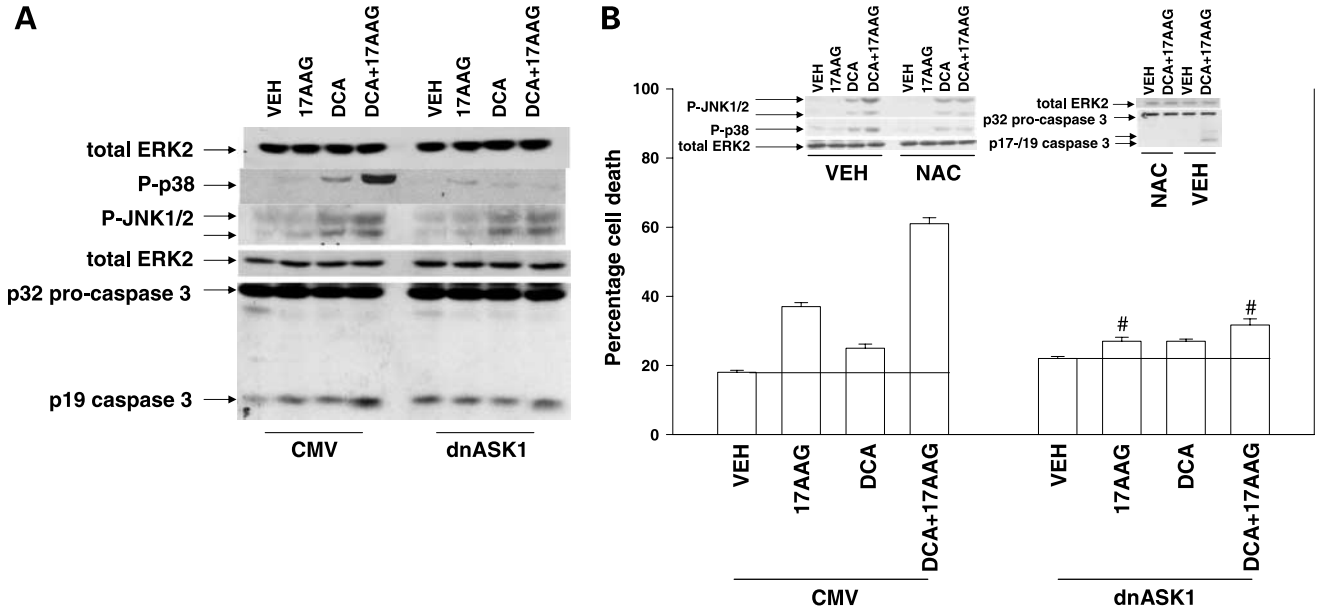

Figure 4. Expression of dominant-negative ASK1 or incubation with ROS-quenching agents suppressed the enhanced activation of JNK1/2 and p38 MAPK by 17AAG and DCA exposure and abolished the promotion of cell killing. **A,** primary rat hepatocytes were cultured as in Materials and Methods in 12-well plates and, 4 h after plating, infected (250 MOI) with control (*CMV*) plasmid adsorbed polylysine adenovirus or a dominant-negative ASK1 (*dnASK1*) plasmid adsorbed virus. Twenty-four hours after infection, cells were treated with vehicle, 17AAG (1 μmol/L), DCA (50 μmol/L), or 17AAG and DCA. Cells were isolated 4 h after exposure, and immunoblotting was done to determine the phosphorylation status of JNK1/2 and p38 MAPK and the expression of procaspase-3 and cleaved caspase-3. Data are from a representative study ($n = 3$). **B,** primary rat hepatocytes were cultured as in Materials and Methods in 12-well plates and, 4 h after plating, infected (250 MOI) with control (*CMV*) plasmid adsorbed polylysine adenovirus or a dominant-negative ASK1 plasmid adsorbed virus. Twenty-four hours after infection, cells were treated with vehicle, 17AAG (1 μmol/L), DCA (50 μmol/L), or 17AAG and DCA. Cells were isolated 4 h after exposure by trypsinization 4 h after DCA/17AAG exposure and spun onto glass slides. Cells were stained with Wright-Giemsa, and the total number of dead (apoptotic and necrotic) cells was determined as a percentage of all cells counted. *Columns,* each assay was done in triplicate ($n = 3$); *bars,* SE. #, $P < 0.05$, less than corresponding treatment value in vector-transfected cells. *Inset,* primary rat hepatocytes were cultured as in Materials and Methods in 12-well plates and, 24 h after plating, treated with vehicle (DMSO) or NAC (20 mmol/L). Thirty minutes after NAC treatment, hepatocytes were treated with vehicle (DCA, PBS; 17AAG, DMSO), 17AAG (1 μmol/L), DCA (50 μmol/L), or the combination of the agents. Cells were isolated 2 h after exposure (*P-JNK1/2* and *P-p38*) or 4 h after exposure (*caspase 3*), and immunoblotting was done to determine the phosphorylation status of JNK1/2 and p38 MAPK. Data are from a representative study ($n = 3$).

inhibitor combined with 17-dimethylaminoethylamino-17-demethoxygeldanamycin.[7] In primary hepatocytes, we have previously published that DCA-induced ERK1/2 activation is suppressed by inhibition of PI3K, and in agreement with these prior findings, inhibition of PI3K function also promoted 17AAG- and DCA-induced cell death (25).

As cell killing was ROS dependent and required activation of both the JNK1/2 and the p38 MAPK pathways, we next investigated whether a ROS-sensitive kinase, previously determined in other cell types to be a ROS-dependent upstream activator of the p38 MAPK and JNK1/2 pathways, apoptosis signaling kinase 1 (ASK1), was involved in promoting p38 MAPK and JNK1/2 activation and altering the survival response to DCA and 17AAG exposure. Expression of dominant-negative ASK1 did not reduce the activation of JNK1/2 induced by DCA but suppressed the enhanced level of JNK1/2 activation induced by combined DCA and 17AAG exposure (Fig. 4A). Expression of dominant-negative ASK1 abolished the activation of p38 MAPK induced either by DCA or by combined DCA and 17AAG exposure and reduced procaspase-3 cleavage (Fig. 4A). Dominant-negative ASK1 reduced the lethality of 17AAG as a single agent and abolished the enhancement of 17AAG lethality caused by DCA (Fig. 4B). Treatment of hepatocytes with ROS-quenching agents did not alter DCA-induced activation of either p38α MAPK or JNK1/2 but suppressed the enhanced levels of p38α MAPK and JNK1/2 activation observed in cells treated with DCA and 17AAG (Fig. 4B, *inset*).

To further illustrate the immunoblotting data in Fig. 4B, in the presence of vehicle, DCA activated JNK1/2 2.2 ± 0.5–fold above basal levels and combined exposure to DCA and 17AAG activated JNK1/2 6.8 ± 1.6–fold above basal levels; this represents a 4.8-fold increase in DCA-stimulated JNK1/2 activity caused by 17AAG coexposure ($n = 3$; $P < 0.05$ greater activation for the combined exposure than the fold activation induced by either agent alone). In contrast, in the presence of NAC, DCA activated JNK1/2 2.0 ± 0.6–fold above basal levels and combined exposure to DCA and

[7] Unpublished observations.

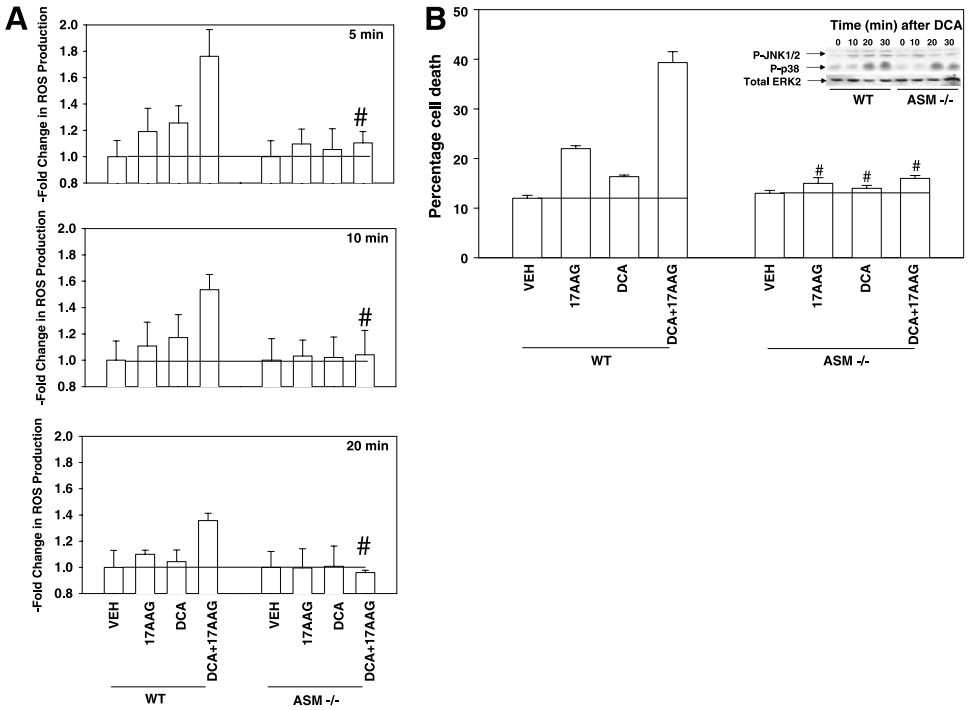

Figure 5. ROS production after 17AAG and DCA exposure is dependent on expression of acidic sphingomyelinase. **A,** primary mouse hepatocytes [wild-type (*WT*); acidic sphingomyelinase null (*ASM*$^{-/-}$)] were cultured as in Materials and Methods in 96-well plates and, 24 h after plating, simultaneously treated where appropriate with vehicle (DCA, PBS; 17AAG, DMSO), 17AAG (1 μmol/L), DCA (50 μmol/L), or the combination of the agents. Before each indicated time point, DCFH was added to the culture medium as described in Materials and Methods. Medium containing the dye was removed after 15 min, and fresh medium that did not contain any agent was added. Plates were immediately placed into an appropriate plate reader to determine DCFH fluorescence. *Columns,* mean of eight separate determinations from one representative experiment ($n = 3$); *bars,* SE. #, $P < 0.05$, less than corresponding treatment value in vector-transfected cells. **B,** primary mouse hepatocytes [wild-type (*WT*); acidic sphingomyelinase null (*ASM*$^{-/-}$)] were cultured as in Materials and Methods in 12-well plates, and 24 h after plating, cells were treated with vehicle, 17AAG (1 μmol/L), DCA (50 μmol/L), or 17AAG and DCA. Cells were isolated by trypsinization 4 h after DCA/17AAG exposure and spun onto glass slides. Cells were stained with Wright-Giemsa, and the total number of dead (apoptotic and necrotic) cells was determined as a percentage of all cells counted. *Columns,* each assay was done in triplicate ($n = 3$); *bars,* SE. #, $P < 0.05$, less than corresponding treatment value in wild-type cells. *Inset,* immunoblotting was done 0 to 30 min after exposure to determine the phosphorylation status of JNK1/2 and p38 MAPK. Data are from a representative study ($n = 3$).

17AAG activated JNK1/2 2.3 ± 0.5–fold above basal levels; this represents a 1.3-fold increase in DCA-stimulated JNK1/2 activity caused by 17AAG coexposure ($P < 0.05$ for less JNK1/2 activation for combined exposure in the presence of NAC).

With respect to p38 MAPK activation, in the presence of vehicle, DCA activated p38 MAPK 1.8 ± 0.3–fold above basal levels and combined exposure to DCA and 17AAG activated p38 MAPK 2.7 ± 0.4–fold above basal levels; this represents a 2.1-fold increase in DCA-stimulated p38 MAPK activity caused by 17AAG coexposure ($n = 3$; $P < 0.05$ greater activation for the combined exposure than the fold activation induced by either agent alone). In contrast, in the presence of NAC, DCA activated p38 MAPK 1.5 ± 0.3–fold above basal levels and combined exposure to DCA and 17AAG activated p38 MAPK 1.8 ± 0.5–fold above basal levels; this represents a 1.6-fold increase in DCA-stimulated p38 MAPK activity caused by 17AAG coexposure ($P < 0.05$ for less p38 MAPK activation by the combination of agents in the presence of NAC). A nonsignificant trend of NAC inhibiting DCA-induced p38 MAPK activation was noted. Collectively, these findings argue that, after DCA and 17AAG treatment, ROS, signaling in part via ASK1, cause a prolonged intense activation of the p38 MAPK and JNK1/2 pathways for at least 2 h, which are responsible for subsequent enhanced levels of primary hepatocyte cell death.

In prior studies, we have shown in primary mouse hepatocytes lacking acidic sphingomyelinase expression that bile acids no longer enhance ceramide production and cannot activate JNK1/2 (30). Treatment of primary rat hepatocytes with DCA, but not 17AAG, also enhanced ceramide production after DCA exposure (data not shown). In hepatocytes derived from acidic sphingomyelinase–null (−/−) mice, ROS generation induced by DCA and 17AAG, either as single agents or when used in combination, was abolished (Fig. 5A). Furthermore, in mouse acidic sphingomyelinase (−/−) hepatocytes, cell killing caused by either DCA or 17AAG as single agents or when used in combination was significantly reduced; of note, inhibitors of *de novo* ceramide synthesis (e.g., fumonisin B1) did not alter the apoptotic response of hepatocytes to either agent (Fig. 5B; data not shown). These findings correlated with an acidic sphingomyelinase–dependent JNK1/2 activation,

but not p38 MAPK activation, in primary mouse hepatocytes within 30 min of bile acid exposure (Fig. 5B, *inset*). Collectively, our findings in Figs. 2 to 5 show that (*a*) activation of JNK1/2 but not p38 MAPK by DCA requires acidic sphingomyelinase expression, (*b*) the prolonged intense activation of p38 MAPK and JNK1/2 caused by combined DCA and 17AAG exposure is ROS dependent, and (*c*) acidic sphingomyelinase expression is required for DCA and 17AAG to promote ROS generation and for ROS to cause prolonged intense activation of the p38 MAPK and JNK1/2 pathways.

Based on the above findings, we next determined the molecular mechanisms by which DCA and 17AAG interacted to cause hepatocyte death. Prior studies by our group have shown that DCA lethality as a single agent, and DCA lethality that was enhanced by MEK1/2/PI3K inhibitors, was dependent on ligand-independent activation of the FAS death receptor (CD95), leading to activation of caspase-8, BID cleavage, mitochondrial dysfunction with cytochrome *c* release into the cytosol, and cell killing. Inhibition of caspase-8 function or expression of dominant-negative FAS-associated death domain weakly suppressed the lethality of DCA and 17AAG (Fig. 6A; data not shown). In contrast, inhibition of caspase-9 function abolished the lethal effects of DCA and 17AAG (Fig. 6A). Overexpression of BCL-$_{XL}$ abolished DCA- and 17AAG-induced cell killing (Fig. 6B). In general agreement with DCA and 17AAG promoting activation of the intrinsic apoptosis pathway, DCA and 17AAG treatment promoted a rapid release of cytochrome *c* from mitochondria that was blocked by ROS-quenching agents, by expression of constitutively active AKT, and by expression of either dominant-negative JNK1 or dominant-negative p38α MAPK (Fig. 6B, *inset*). Treatment of primary rat hepatocytes with DCA and 17AAG promoted the association of BAX with hepatocyte mitochondria, an effect that was blocked by expression of constitutively active AKT (Fig. 6B, *inset*). These findings suggest that activated AKT suppresses activation of the intrinsic apoptosis pathway via blockade of JNK1/2 pathway activation and by inhibition of BAX association with mitochondria.

To further define the mechanisms of cell killing, we made use of transformed MEFs lacking expression of various proapoptotic proteins. Treatment of SV40-transformed MEFs with DCA and 17AAG caused a greater than additive increase in cell killing within 12 h of treatment, which was of a similar quantitative level to that observed in primary rodent hepatocytes 4 h after drug treatment; loss of BAK

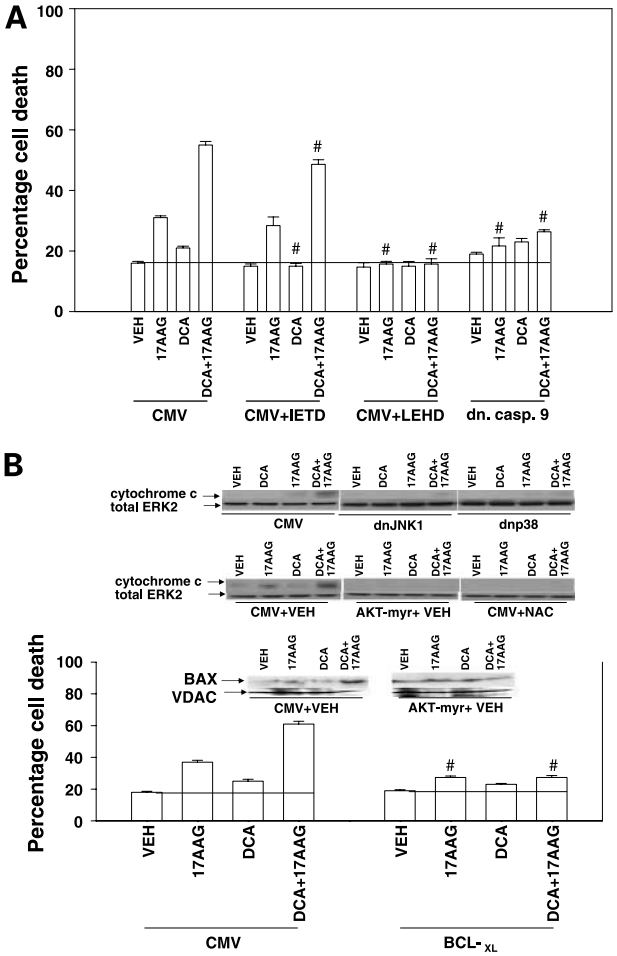

Figure 6. DCA and 17AAG promote hepatocyte cell killing through a mitochondrial (intrinsic) apoptosis-dependent pathway. **A,** primary rat hepatocytes were cultured as in Materials and Methods in 12-well plates and, 4 h after plating, infected (50 MOI) with control (*CMV*) recombinant adenovirus or a dominant-negative caspase-9 virus (*dn. casp. 9*). Twenty-four hours after infection, cells were treated with vehicle, caspase-8 inhibitor IETD (50 μmol/L), or caspase-9 inhibitor LEHD (50 μmol/L). After 30 min, cells were treated with vehicle (DCA, PBS; 17AAG, DMSO), 17AAG (1 μmol/L), DCA (50 μmol/L), or the combination of the agents. Cells were isolated by trypsinization 4 h after DCA/17AAG exposure and spun onto glass slides. Cells were stained with Wright-Giemsa, and the total number of dead (apoptotic and necrotic) cells was determined as a percentage of all cells counted. *Columns,* each assay was done in triplicate and the data are from a representative study done by two different individuals (n = 3); *bars,* SE. #, $P < 0.05$, less than corresponding treatment value in vector-transfected cells. **B,** primary rat hepatocytes were cultured as in Materials and Methods in 12-well plates and, 4 h after plating, infected (50 MOI) with control (*CMV*) recombinant adenovirus or a virus to express BCL-$_{XL}$. Twenty-four hours after infection, cells were treated with vehicle (DCA, PBS; 17AAG, DMSO), 17AAG (1 μmol/L), DCA (50 μmol/L), or the combination of the agents. Cells were isolated by trypsinization 4 h after DCA/17AAG exposure and spun onto glass slides. Cells were stained with Wright-Giemsa, and the total number of dead (apoptotic and necrotic) cells was determined as a percentage of all cells counted. *Columns,* each assay was done in triplicate and data are from a representative study done by two different individuals (n = 3); *bars,* SE. #, $P < 0.05$, less than corresponding treatment value in vector-transfected cells. *Inset,* primary rat hepatocytes were cultured as in Materials and Methods in 12-well plates and, 4 h after plating, infected (50 MOI) with control (*CMV*) recombinant adenovirus or viruses to express activated AKT, dominant-negative JNK1, or dominant-negative p38α MAPK. In parallel sets of CMV virus–infected plates, cells were treated ~24 h after infection with NAC (20 mmol/L). Twenty-four hours after infection, cells were treated with vehicle (DCA, PBS; 17AAG, DMSO), 17AAG (1 μmol/L), DCA (50 μmol/L), or the combination of the agents. Cells were isolated by trypsinization 2 h after DCA/17AAG exposure, and the cytosolic and crude granular fractions were isolated. Protein lysates were subjected to SDS-PAGE followed by immunoblotting to detect the protein levels of BAX, cytochrome *c*, ERK2, and voltage-dependent anion channel (*VDAC*) in each fraction (n = 3).

function weakly suppressed 17AAG and DCA lethality, whereas loss of BAX function significantly suppressed cell death (Fig. 7A and B). Deletion of both BAX and BAK expression abolished the ability of DCA and 17AAG to cause fibroblast cell death (Fig. 7A and B). In agreement with our data showing that inhibition of caspase-8 function modestly suppressed DCA and 17AAG lethality in primary hepatocytes, loss of BID function did not significantly alter the death response of DCA- and 17AAG-treated cells.

As 17AAG blocks HSP90 function, which in turn causes an unfolded protein stress response that can lead to cell death, we determined whether loss of PERK function modified the toxicity of DCA and 17AAG exposure (reviewed in refs. 33–35 and references therein). PERK can play an important role in sensing an increase of misfolded proteins within the ER (33–35). Loss of PERK function suppressed the apoptotic response of fibroblasts exposed to 17AAG and to DCA and 17AAG (Fig. 7B). Based on our findings in PERK$^{-/-}$ cells with respect to 17AAG toxicity, we investigated whether loss of PERK signaling altered the ability of 17AAG and DCA to increase ROS levels. Loss of PERK function suppressed ROS generation by 17AAG and by combined 17AAG and DCA exposure (Fig. 7C).

PERK is localized in the ER, and changes in ER function, including the release of Ca^{2+} from the ER into the cytosol, have been argued by others to modulate mitochondrial function and ROS production (35–37). Furthermore, changes in Ca^{2+} have also been linked to ROS production by mitochondria (35). Thus, based on our data showing that the ability of 17AAG to enhance DCA-induced ROS

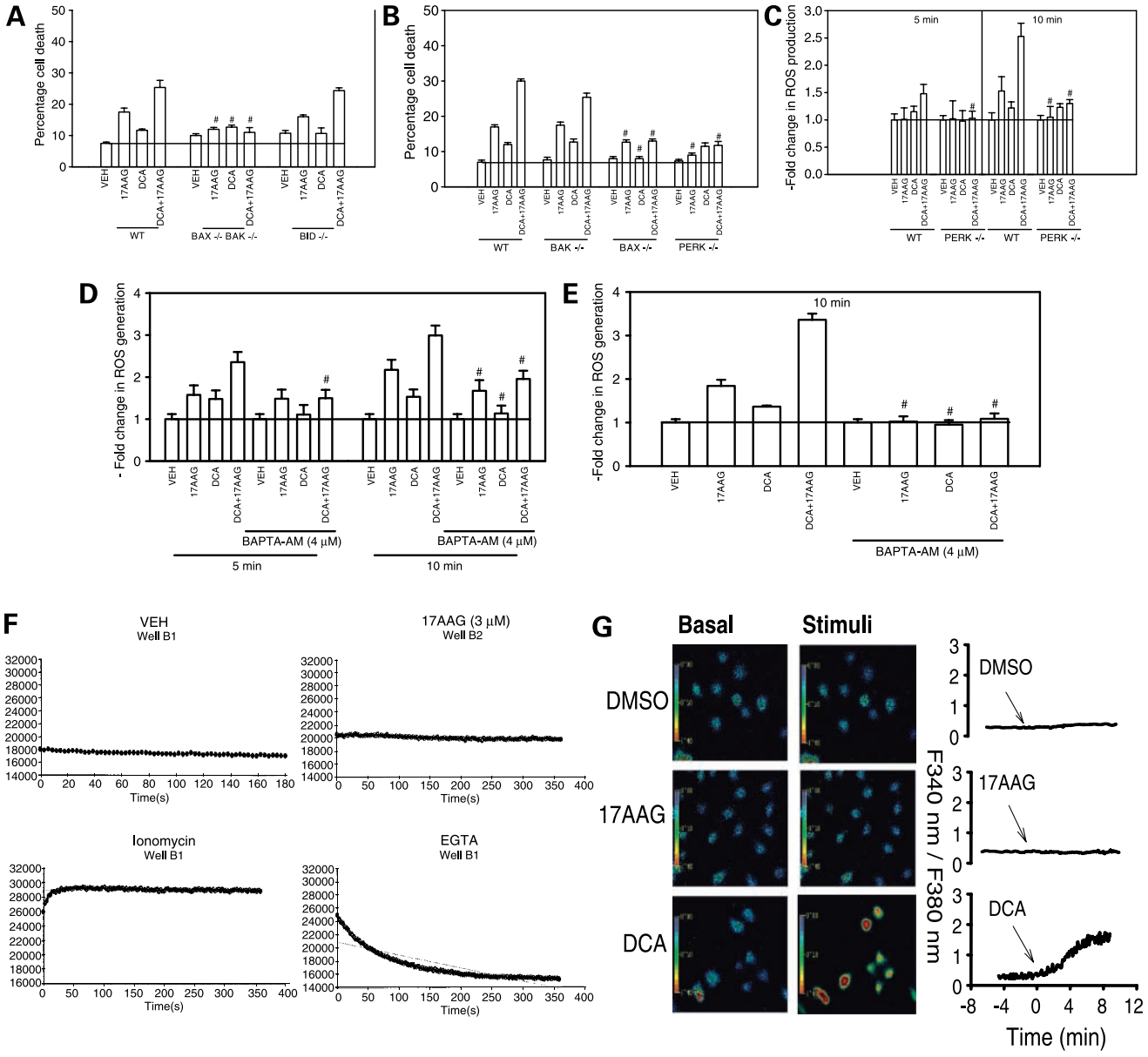

generation was PERK dependent, we next investigated whether changes in intracellular Ca^{2+} levels were responsible for the PERK-dependent regulation of ROS production. The enhanced level of ROS production induced by combined DCA and 17AAG treatment was significantly suppressed when transformed fibroblasts or primary hepatocytes were incubated in Ca^{2+}-free medium and in the presence of the intracellular chelator BAPTA-AM (Fig. 7D and E). Despite other studies arguing that treatment of cells with geldanamycins can enhance cytosolic Ca^{2+} levels, we did not note any alteration in intracellular Ca^{2+} levels after 17AAG exposure in MEFs (Fig. 7F and G; ref. 38). In contrast to 17AAG, treatment with DCA promoted modest changes in cytosolic Ca^{2+} levels in MEFs; however, treatment of cells with 17AAG and DCA did not alter the enhanced level of Ca^{2+} release compared with DCA treatment alone (Fig. 7G; data not shown).

Discussion

Previous studies have shown that geldanamycins have dose-limiting toxicity *in vivo* due to their actions in promoting liver dysfunction (e.g., ref. 19). The present studies were initiated to better understand how hepatotoxicity of geldanamycins could be ameliorated to improve the therapeutic index of these agents.

The majority of published studies with regard to toxic geldanamycin actions are based on the fact that ansamycin antibiotics suppress the function of HSP90, thereby promoting the degradation and ultimate inhibition of kinase signaling (e.g., ERBB2, BCR-ABL, Raf-1, B-Raf, and AKT), which function in a wide variety of tumor cells to promote cell growth and cell survival. In addition, it has been noted that mutated active forms of such kinases (e.g., BCR-ABL and B-Raf) in tumor cells have a higher rate of degradation following HSP90 inhibition than nonmutated forms of the same proteins (e.g., ref. 16). In primary hepatocytes, however, which have low basal activities of kinases within all signaling pathways, we noted that 17AAG did not prevent DCA from activating MEK1/2, ERK1/2, or AKT within a 6-h time frame and within 6 h of 17AAG treatment and Raf-1 protein levels in hepatocytes remained constant; yet, 17AAG as a single agent and when combined with DCA caused significant amounts of hepatocyte cell killing. Of note, as single agents, 17AAG generated less ROS than DCA but caused significantly more hepatocyte death. Combined treatment with 17AAG and DCA caused an enhanced activation of both the p38 MAPK and the JNK1/2 pathways, and activation of both the p38 MAPK and the JNK1/2 pathways was required for manifestation of the cytotoxic effects of combined 17AAG and DCA treatment. The proapoptotic signaling effects of JNK1/2 and p38 MAPK occurred within ~2 h of drug exposure as judged by mitochondrial dysfunction, caspase activation, and nuclear morphology, indicative of cell death. Our findings argue that at least a portion of 17AAG toxicity and of 17AAG and DCA toxicity in primary hepatocytes, on initial exposure to the drug and bile acid, may be due to mechanisms independent

Figure 7. DCA and 17AAG promote cell killing through a PERK- and BAX/BAK-dependent pathway. **A,** transformed MEFs [wild-type (*WT*), lacking BAX and BAK (*BAX−/− BAK−/−*), and lacking BID (*BID−/−*)] were cultured as in Materials and Methods in 12-well plates, and 24 h after plating, cells were treated with vehicle (DCA, PBS; 17AAG, DMSO), 17AAG (1 μmol/L), DCA (50 μmol/L), or the combination of the agents. Cells were isolated by trypsinization 12 h after DCA/17AAG exposure and spun onto glass slides. Cells were stained with Wright-Giemsa, and the total number of dead (apoptotic and necrotic) cells was determined as a percentage of all cells counted. *Columns,* each assay was done in triplicate and the data are from a representative study done by two different individuals ($n = 3$); *bars,* SE. #, $P < 0.05$, less than corresponding treatment value in vector-transfected cells. **B,** transformed MEFs [wild-type (*WT*), *BAK−/−*, *BAX−/−* , and *PERK−/−*)] were cultured as in Materials and Methods in 12-well plates, and 24 h after plating, cells were treated with vehicle (DCA, PBS; 17AAG, DMSO), 17AAG (1 μmol/L), DCA (50 μmol/L), or the combination of the agents. Cells were isolated by trypsinization 12 h after DCA/17AAG exposure and spun onto glass slides. Cells were stained with Wright-Giemsa, and the total number of dead (apoptotic and necrotic) cells was determined as a percentage of all cells counted. *Columns,* each assay was done in triplicate and the data are from a representative study done by two different individuals ($n = 3$); *bars,* SE. #, $P < 0.05$, less than corresponding treatment value in vector-transfected cells. **C,** transformed MEFs (*WT* and *PERK−/−*) were cultured as in Materials and Methods in 96-well plates and, 24 h after plating, simultaneously treated where appropriate with vehicle (DCA, PBS; 17AAG, DMSO), 17AAG (1 μmol/L), DCA (50 μmol/L), or the combination of the agents. Fifteen minutes before each indicated time point, DCFH was added to the culture medium as described in Materials and Methods. Medium containing the dye was removed, and fresh medium that did not contain any agent was added. Plates were immediately placed into an appropriate plate reader to determine DCFH fluorescence. *Columns,* mean of eight separate determinations from one representative experiment ($n = 3$ experiments); *bars,* SE. #, $P < 0.05$, less than corresponding treatment value in vector-transfected cells. **D,** transformed MEFs were cultured in either DMEM or Ca^{2+}-free DMEM containing 2 mmol/L BAPTA-AM as in Materials and Methods in 96-well plates and, 24 h after plating, simultaneously treated where appropriate with vehicle (DCA, PBS; 17AAG, DMSO), 17AAG (1 μmol/L), DCA (50 μmol/L), or the combination of the agents. Fifteen minutes before each indicated time point, DCFH was added to the culture medium as described in Materials and Methods. Medium containing the dye was removed, and fresh medium that did not contain any agent was added. Plates were immediately placed into an appropriate plate reader to determine DCFH fluorescence. *Columns,* mean of eight separate determinations from one representative experiment ($n = 3$); *bars,* SE. #, $P < 0.05$, less than corresponding treatment value in complete medium cells. **E,** primary rat hepatocytes were cultured in either DMEM or Ca^{2+}-free DMEM containing 2 mmol/L BAPTA-AM as in Materials and Methods in 96-well plates and, 24 h after plating, simultaneously treated where appropriate with vehicle (DCA, PBS; 17AAG, DMSO), 17AAG (1 μmol/L), DCA (50 μmol/L), or the combination of the agents. Fifteen minutes before each indicated time point, DCFH was added to the culture medium as described in Materials and Methods. Medium containing the dye was removed, and fresh medium that did not contain any agent was added. Plates were immediately placed into an appropriate plate reader to determine DCFH fluorescence. *Columns,* mean of eight separate determinations from one representative experiment ($n = 3$); *bars,* SE. #, $P < 0.05$, less than corresponding treatment value in complete medium cells. **F,** cells were stimulated with either vehicle [DMSO; final concentration, 0.15% (v/v)], 17AAG (3 mmol/L), EGTA (5 mmol/L), and ionomycin (10 μg/mL), and the fluorescence was monitored over time on a Bio-Tek FL600 fluorescence/absorbance spectophotometer. The wavelength for excitation was 485 nm and emission was measured at 530 nm. **G,** MEFs, seeded on the four-well chamber with a transparent bottom (Lab-Tek), with fura-2 as an indicator. After loading with 10 μmol/L fura-2 at room temperature for 50 min, the cells were washed thrice with Hanks' buffer at pH 7.4. Then, 17AAG (3 μmol/L), DCA (50 μmol/L), or combination of 17AAG (3 μmol/L) and DCA (50 μmol/L) was added into the bath solution to stimulate the MEFs, respectively. Data are from a representative experiment ($n = 4$).

of suppressing HSP90 function. As many tumor cell types are exquisitely sensitive to suppression of HSP90 function and deregulation of survival signaling pathways, our data suggest that the initial suppression of geldanamycin plus bile acid–induced ROS production in the liver could be a strategy to ameliorate geldanamycin hepatotoxicity in patients.

We tested whether modulation of MEK1/2 and AKT signaling could alter cell survival. Expression of constitutively active AKT reduced the toxicity both of 17AAG and of DCA and 17AAG, treatment that correlated with a modest reduction in the total JNK1/2 activity as well as with suppression of the enhanced JNK1/2 activation following DCA and 17AAG exposure. Thus, a portion of the protective effect of activated AKT may be due to a suppression of JNK1/2 signaling. Constitutively active AKT did not alter p38 MAPK activation under any treatment/condition; p38 MAPK activation was ASK1 dependent, arguing that under our culture conditions AKT is not regulating ASK1 function in primary rat hepatocytes. Activated MEK1, but not active AKT, suppressed the modest levels of DCA toxicity we observed but had no effect on cell survival after DCA and 17AAG treatment. These findings suggest that 17AAG either inhibits protective MEK1/2-ERK1/2 signaling at a site downstream of these kinases or recruits signaling pathways to kill hepatocytes whose proapoptotic functions cannot be suppressed by activated MEK1.

In contrast to data using activated constructs of AKT and MEK1, expression of dominant-negative MEK1 or treatment with the PI3K inhibitor LY294002, but not expression of dominant-negative AKT, significantly enhanced the lethality of both DCA and DCA and 17AAG treatment. Prior articles from this group have shown that inhibition of PI3K blocks bile acid–induced activation of both ERK1/2 and AKT and, together with our present findings, argues that DCA-induced and DCA and 17AAG–induced compensatory activation of the PI3K/MEK1/2/ERK1/2 pathway plays a greater role in maintaining cell viability than activation of the PI3K/AKT pathway. That is, MEK1/2-ERK1/2 signaling represents the key initial endogenous compensatory protective signaling response for hepatocellular survival after DCA and 17AAG exposure.

In one study using hematopoietic cells, geldanamycins have been argued to mediate their toxicity, in part, by causing the generation of ROS (e.g., ref. 5). In primary rat hepatocytes and HuH7 human hepatoma cells, 17AAG modestly increased ROS levels within 30 min of exposure. In primary rat hepatocytes, DCA and 17AAG interacted to promote significantly higher peak levels of ROS production and the duration of ROS production was at least tripled (from ~20 min to +60 min). Phenomenologically similar, although more modest, ROS generation after treatment with these agents was observed in primary mouse hepatocytes. Production of ROS was dependent on functional mitochondria based on a loss of ROS production in Rho 0 cells and by use of the drugs cyclosporin A and bongkrekic acid. Suppression of ROS levels using small molecule and molecular approaches following DCA and 17AAG exposure blunted the elevated and prolonged activation of both the p38 MAPK and the JNK1/2 signaling modules as well as the induction of cell killing. These findings argue that the toxic interaction of 17AAG with DCA is dependent on prolonged high levels of ROS generation by mitochondria but that 17AAG lethality as a single agent in hepatocytes has both ROS-dependent and ROS-independent components. As hepatocytes invariably interact with geldanamycins *in vivo* in the presence of bile acids, and hepatocytes have been reported to contain significantly more mitochondria per cell than many other nontransformed and transformed cell types, our findings with respect to ROS generation also likely explain why the liver is a site of dose-limiting toxicity for geldanamycins (39).

Previous articles from our group have shown that bile acid–induced activation of JNK1/2 in hepatocytes is dependent on increased ceramide levels and not on ROS generation, ceramide generation being reliant on the activation of acidic sphingomyelinase (30). As 17AAG and DCA promoted JNK1/2 activation, we examined the effect of acidic sphingomyelinase function on 17AAG and DCA toxicity. In our studies, 17AAG did not seem to generate significant amounts of ceramide. However, loss of acidic sphingomyelinase function reduced JNK1/2 activation under all treatment conditions, which correlated with lower levels of cell killing following 17AAG, DCA, and 17AAG and DCA exposure. Loss of acidic sphingomyelinase function reduced the ability of DCA and 17AAG to generate ROS. Thus, in addition to confirming our prior findings with DCA, the present studies argue that 17AAG lethality as a single agent in hepatocytes requires acidic sphingomyelinase function and that acidic sphingomyelinase function is also required for the generation of ROS by bile acids.

Inhibition of HSP90 function causes increased levels of unfolded proteins within the ER, and because of this, we determined whether a kinase involved in ER stress signaling, PERK, was involved in the lethality of 17AAG. Loss of PERK function reduced 17AAG lethality by >80% in transformed fibroblasts 12 h after drug exposure and also abolished the lethal interaction between DCA and 17AAG. Because of our findings in hepatocytes, which argued that one primary effect of 17AAG exposure was to promote ROS generation, we investigated whether loss of PERK function altered the ability of 17AAG to increase ROS levels. Somewhat to our surprise, the ROS generation that was induced within 10 min of DCA and 17AAG exposure was blocked in $PERK^{-/-}$ cells. Marcu et al. (12) showed that HSP90 binds to PERK and that geldanamycin promotes HSP90 dissociation from PERK, causing PERK expression to decline over several hours; these studies also stated that geldanamycin did not prevent an ER stressor from causing PERK autophosphorylation. Using commercially available anti–phosphorylated PERK antibodies, we were unable to detect changes in PERK autophosphorylation in any of our studies within this article (data not shown). Whether the

initial prompt effect of 17AAG on HSP90 function, or on the function of the ER HSP90 analogue Grp94, results in PERK activation in hepatocytes will require additional future studies.

The ER is a major store of intracellular Ca^{2+}, and release of stored Ca^{2+} into the cytosol has been noted by others to promote mitochondrial ROS production (37–39). Treatment of cells with 17AAG promoted a rapid increase in ROS levels, and 17AAG-induced ROS levels were suppressed in cells incubated in Ca^{2+}-free medium and the chelator BAPTA-AM. DCA caused cytosolic release of Ca^{2+}; however, 17AAG was unable to alter Ca^{2+} levels using two different systems to measure Ca^{2+} release. Thus, in contrast to the findings of Chang et al. who used the parent compound geldanamycin to alter Ca^{2+} levels, 17AAG did not alter Ca^{2+} levels but, in a Ca^{2+}-dependent fashion, played an essential role in mitochondrial-dependent ROS generation that leads to cell death. Additional studies outside the scope of the present article will be required to determine the precise role of Ca^{2+} in the interaction between DCA and 17AAG.

In conclusion, our studies have argued that prolonged ROS generation by combined DCA and 17AAG exposure was a primary causal event in hepatocyte lethality. The use of agents that quench ROS thus has potential to suppress the toxicity of geldanamycins in the liver while still permitting down-regulation of HSP90 client proteins in tumor cells. Further studies will be required to test this utility of this approach.

Acknowledgments

We thank Dr. Sarah Spiegel for assistance with ceramide assays.

References

1. Garrido C, Gurbuxani S, Ravagnan L, Kroemer G. Heat shock proteins: endogenous modulators of apoptotic cell death. Biochem Biophys Res Commun 2001;286:433 – 42.

2. Stancato LF, Silverstein AM, Owens-Grillo JK, Chow YH, Jove R, Pratt WB. The hsp90-binding antibiotic geldanamycin decreases Raf levels and epidermal growth factor signaling without disrupting formation of signaling complexes or reducing the specific enzymatic activity of Raf kinase. J Biol Chem 1997;272:4013 – 20.

3. Stebbins CE, Russo AA, Schneider C, Rosen N, Hartl FU, Pavletich NP. Crystal structure of an Hsp90-geldanamycin complex: targeting of a protein chaperone by an antitumor agent. Cell 1997;89:239 – 50.

4. Nimmanapalli R, O'Bryan E, Bhalla K. Geldanamycin and its analogue 17-allylamino-17-demethoxygeldanamycin lowers Bcr-Abl levels and induces apoptosis and differentiation of Bcr-Abl-positive human leukemic blasts. Cancer Res 2001;61:1799 – 804.

5. Nimmanapalli R, O'Bryan E, Kuhn D, Yamaguchi H, Wang HG, Bhalla KN. Regulation of 17-AAG-induced apoptosis: role of Bcl-2, Bcl-XL, and Bax downstream of 17-AAG-mediated down-regulation of Akt, Raf-1, and Src kinases. Blood 2003;102:269 – 75.

6. Rahmani M, Yu C, Dai Y, et al. Coadministration of the heat shock protein 90 antagonist 17-allylamino-17-demethoxygeldanamycin with suberoylanilide hydroxamic acid or sodium butyrate synergistically induces apoptosis in human leukemia cells. Cancer Res 2003;63:8420 – 7.

7. Jia W, Yu C, Rahmani M, et al. Synergistic antileukemic interactions between 17-AAG and UCN-01 involve interruption of RAF/MEK- and AKT-related pathways. Blood 2003;102:1824 – 32.

8. Rahmani M, Reese E, Dai Y, et al. Cotreatment with suberanoylanilide hydroxamic acid and 17-allylamino 17-demethoxygeldanamycin synergistically induces apoptosis in Bcr-Abl+ cells sensitive and resistant to STI571 (imatinib mesylate) in association with down-regulation of Bcr-Abl, abrogation of signal transducer and activator of transcription 5 activity, and Bax conformational change. Mol Pharmacol 2005;67:1166 – 76.

9. Guo F, Rocha K, Bali P, et al. Abrogation of heat shock protein 70 induction as a strategy to increase antileukemia activity of heat shock protein 90 inhibitor 17-allylamino-demethoxy geldanamycin. Cancer Res 2005;65:10536 – 44.

10. Mimnaugh EG, Xu W, Vos M, et al. Simultaneous inhibition of hsp 90 and the proteasome promotes protein ubiquitination, causes endoplasmic reticulum-derived cytosolic vacuolization, and enhances antitumor activity. Mol Cancer Ther 2004;3:551 – 66.

11. DeBoer C, Meulman PA, Wnuk RJ, Peterson DH. Geldanamycin, a new antibiotic. J Antibiot (Tokyo) 1970;23:442 – 7.

12. Marcu MG, Doyle M, Bertolotti A, Ron D, Hendershot L, Neckers L. Heat shock protein 90 modulates the unfolded protein response by stabilizing IRE1α. Mol Cell Biol 2002;22:8506 – 13.

13. Lawson B, Brewer JW, Hendershot LM. Geldanamycin, an hsp90/GRP94-binding drug, induces increased transcription of endoplasmic reticulum (ER) chaperones via the ER stress pathway. J Cell Physiol 1998;174:170 – 8.

14. Lai MT, Huang KL, Chang WM, Lai YK. Geldanamycin induction of grp78 requires activation of reactive oxygen species via ER stress responsive elements in 9L rat brain tumour cells. Cell Signal 2003;15:585 – 95.

15. Solit DB, Basso AD, Olshen AB, Scher HI, Rosen N. Inhibition of heat shock protein 90 function down-regulates Akt kinase and sensitizes tumors to Taxol. Cancer Res 2003;63:2139 – 44.

16. Grbovic OM, Basso AD, Sawai A, et al. V600E B-Raf requires the Hsp90 chaperone for stability and is degraded in response to Hsp90 inhibitors. Proc Natl Acad Sci U S A 2006;103:57 – 62.

17. Grem JL, Morrison G, Guo XD, et al. Phase I and pharmacologic study of 17-(allylamino)-17-demethoxygeldanamycin in adult patients with solid tumors. J Clin Oncol 2005;23:1885 – 93.

18. Ramanathan RK, Trump DL, Eiseman JL, et al. Phase I pharmacokinetic-pharmacodynamic study of 17-(allylamino)-17-demethoxygeldanamycin (17AAG, NSC 330507), a novel inhibitor of heat shock protein 90, in patients with refractory advanced cancers. Clin Cancer Res 2005;11:3385 – 91.

19. Banerji U, O'Donnell A, Scurr M, et al. Phase I pharmacokinetic and pharmacodynamic study of 17-allylamino, 17-demethoxygeldanamycin in patients with advanced malignancies. J Clin Oncol 2005;23:4152 – 61.

20. Pizzuto J, Aviles A, Ramos E, Cervera J, Aguirre J. Cytosine arabinoside induced liver damage: histopathologic demonstration. Med Pediatr Oncol 1983;11:287 – 90.

21. Wang ZY, Chen Z. arsenic Differentiation and apoptosis induction therapy in acute promyelocytic leukaemia. Lancet Oncol 2000;1:101 – 6.

22. Ohe Y, Niho S, Kakinuma R, et al. Phase I studies of cisplatin and docetaxel administered by three consecutive weekly infusions for advanced non-small cell lung cancer in elderly and non-elderly patients. Jpn J Clin Oncol 2001;31:100 – 6.

23. Roberts MS, Magnusson BM, Burczynski FJ, Weiss M. Enterohepatic circulation: physiological, pharmacokinetic, and clinical implications. Clin Pharmacokinet 2002;41:751 – 90.

24. Poupon R, Chazouilleres O, Poupon RE. Chronic cholestatic diseases. J Hepatol 2000;32:129 – 40.

25. Qiao L, Studer E, Leach K, et al. Deoxycholic acid (DCA) causes ligand-independent activation of epidermal growth factor receptor (EGFR) and FAS receptor in primary hepatocytes: inhibition of EGFR/mitogen-activated protein kinase-signaling module enhances DCA-induced apoptosis. Mol Biol Cell 2001;12:2629 – 45.

26. Fang Y, Han SI, Mitchell C, et al. Bile acids induce mitochondrial ROS, which promote activation of receptor tyrosine kinases and signaling pathways in rat hepatocytes. Hepatology 2004;40:961 – 71.

27. Qiao L, Han SI, Fang Y, et al. Bile acid regulation of C/EBPβ, CREB, and c-Jun function, via the extracellular signal-regulated kinase and c-Jun NH_2-terminal kinase pathways, modulates the apoptotic response of hepatocytes. Mol Cell Biol 2003;23:3052 – 66.

28. Han SI, Studer E, Gupta S, et al. Bile acids enhance the activity of the insulin receptor and glycogen synthase in primary rodent hepatocytes. Hepatology 2004;39:456 – 63.

29. van Montfort RL, Congreve M, Tisi D, Carr R, Jhoti H. Oxidation state of the active-site cysteine in protein tyrosine phosphatase 1B. Nature 2003;423:773 – 7.

30. Gupta S, Natarajan R, Payne SG, et al. Deoxycholic acid activates the c-Jun N-terminal kinase pathway via FAS receptor activation in primary hepatocytes. Role of acidic sphingomyelinase-mediated ceramide generation in FAS receptor activation. J Biol Chem 2004;279:5821 – 8.

31. Merchant NB, Rogers CM, Trivedi B, Morrow J, Coffey RJ. Ligand-dependent activation of the epidermal growth factor receptor by secondary bile acids in polarizing colon cancer cells. Surgery 2005;138: 415 – 21.

32. Werneburg NW, Yoon JH, Higuchi H, Gores GJ. Bile acids activate EGF receptor via a TGF-α-dependent mechanism in human cholangiocyte cell lines. Am J Physiol Gastrointest Liver Physiol 2003;285:G31 – 6.

33. Olivera A, Spiegel S. Ganglioside GM1 and sphingolipid breakdown products in cellular proliferation and signal transduction pathways. Glycoconj J 1992;9:110 – 7.

34. Yacoub A, Park MA, Hanna DJ, et al. OSU-03012 promotes caspase-independent, PERK-, cathepsin B-, BID-, and AIF-dependent killing of transformed cells. Mol Pharmacol 2006;70:589 – 603.

35. Leach JK, Van Tuyle G, Lin PS, Schmidt-Ullrich R, Mikkelsen RB. Ionizing radiation-induced, mitochondria-dependent generation of reactive oxygen/nitrogen. Cancer Res 2001;61:3894 – 901.

36. Ho HK, White CC, Fernandez C, et al. Nrf2 activation involves an oxidative-stress independent pathway in tetrafluoroethylcysteine-induced cytotoxicity. Toxicol Sci 2005;86:354 – 64.

37. Nawaz M, Manzl C, Lacher V, Krumschnabel G. Copper-induced stimulation of ERK in trout hepatocytes: the role of reactive oxygen species, Ca^{2+} and cell energetics and the impact of ERK signalling on apoptosis and necrosis. Toxicol Sci 2006;92:465 – 75.

38. Chang YS, Lee LC, Sun FC, Chao CC, Fu HW, Lai YK. Involvement of calcium in the differential induction of heat shock protein 70 by heat shock protein 90 inhibitors, geldanamycin, and radicicol, in human non-small cell lung cancer H460 cells. J Cell Biochem 2006;97:156 – 65.

39. John GB, Shang Y, Li L, et al. The mitochondrial inner membrane protein mitofilin controls cristae morphology. Mol Biol Cell 2005;16: 1543 – 54.